Chimera method applied to the simulation of a freely falling cylinder in a channel

Thibaut Deloze — Yannick Hoarau — Jan Dušek

Institut des Mécaniques des Fluides et des Solide (IMFS)
Université de Strasbourg
2 rue de Boussingault
F-67000 Strasbourg
deloze@imfs.u-strasbg.fr

ABSTRACT. *In this paper, we study the motion of a circular cylinder freely falling in a channel under the action of gravity parallel to the wall. The fixed parameters of the study are the cylinder diameter to channel width ratio, $D/d = 3.3$, and the fluid to particle density ratio, $\beta = 2$. The varying parameters are the initial position (in or out of the middle axis) and the Galileo number ($151 \leq Ga \leq 300$). An automatic chimera method is implemented in a Navier-Stokes solver to simulate this moving confined configuration. The presence of the wall accelerates the oscillations of the motion. The initial position has an influence on the amplification of transverse oscillations. If the cylinder is out of the middle axis, transverse oscillations appear earlier and reach rapidly the amplitude of the terminal periodic oscillations. A relation between the Strouhal and Reynolds numbers is proposed.*

RÉSUMÉ. *Dans cet article, nous étudions le mouvement d'un cylindre en chute libre dans un canal sous l'action du champ de gravité parallèle aux parois. Les paramètres fixes sont le rapport entre le diamètre du cylindre et la largeur du canal ($D/d = 3{,}3$), puis le rapport entre la densité du fluide et celle de la particule ($\beta = 2$). Les paramètres variants sont la position initiale (sur l'axe médian ou hors de cet axe) et le nombre de Galilée ($151 \leq Ga \leq 300$). Une méthode chimère automatique est mise en place dans un solveur des équations de Navier-Stokes pour simuler cette configuration mobile confinée. Les parois du canal accélèrent les oscillations du mouvement du cylindre. La position initiale a une influence sur l'amplification des oscillations transverses. Si la particule est hors du plan médian, l'oscillation transverse apparaît plus tôt et atteint plus rapidement son amplitude finale. Une relation entre le nombre de Strouhal et le nombre de Reynolds est proposée.*

KEYWORDS: *chimera method, overlapped grid, falling, cylinder, channel.*

MOTS-CLÉS : *méthode chimère, maillage superposé, chute libre, cylindre, canal.*

DOI:10.3166/EJCM.19.575-590

1. Introduction

We are interested in the influence of the vortex shedding on the fall of a particle in a sedimentation problem. In this paper we focus on the free fall of a circular cylinder between two vertical walls. The latter is dominated by the well-known vortice shedding in the cylinder wake. The understanding of vortex dynamics in the cylinder wake is due to several works (Tritton, 1959; Braza *et al.*, 1986; Dušek *et al.*, 1994; Persillon *et al.*, 1998; Williamson *et al.*, 1998). The flow around the cylinder becomes unsteady with the Von Kármán vortex shedding at the Reynolds number of 46. The oscillating wake leads to the oscillation of the induced force in a cross flow direction. The vortex shedding can induce an oscillatory response of a structure (Govardhan *et al.*, 2000; Shiels *et al.*, 2001; Placzek *et al.*, 2009) and a cross flow motion of the cylinder can control the vortex shedding frequency (Koopmann, 1967; Williamson *et al.*, 1988; Anagnostopoulos, 2000; Nobari *et al.*, 2006; Placzek *et al.*, 2009).

A fairly complete numerical investigative of the free fall of cylindrical bodies between vertical walls was presented by Feng et al. ((Feng *et al.*, 1994)). They evidence several regimes in the interval of terminal Reynolds numbers up to 600. They consider a circular and an elliptic cross-section of the cylinder and they tackle even the simultaneous fall of two bodies. Their investigation does not, however, recognise the role of the Galileo number and does not mention the solid/fluid density ratio of the simulation. This limits the quantative relevance of their results.

Jenny et al. (Jenny *et al.*, 2004) studied the free fall of an unconfined spherical particle. They characterized the problem of a fall caused by gravity by two parameters, the density ratio $\beta = \rho/\rho_b$ (with ρ_b the density of the particle and ρ the fluid density) and the Galileo number $Ga = \sqrt{gd^3\rho(\rho_b - \rho)/(\mu^2)}$ (with g the gravity force, d the particle diameter and μ the dynamic viscosity). Their numerical and experimental studies focused on the falling or rising sphere with the identification of different kinds of trajectories depending the both parameters (Ga, β). Horowitz and Williamson (Horowitz *et al.*, 2006) studied experimentally a falling or rising cylinder and showed that the transverse amplitude of the falling cylinder motion is about 5% of the diameter of the cylinder for a density ratio about 1.4 and 2.0. Recently Namkoong et al. (Namkoong *et al.*, 2008) took up the two-dimensional numerical simulation of the free fall of an unconfined cylinder. They focused their work on the frequency of the trajectory for $Ga < 163$ i.e. the terminal $Re < 188$. The vortex shedding causes a periodic transverse displacement of the cylinder. Namkoong et al. related its Strouhal number to the Reynolds number by a simple formula.

We have performed a numerical study of a falling particle under the action of gravity field. The configuration is similar to that of Feng et al. (Feng *et al.*, 1994) : a freely falling cylinder with a diameter d in a channel of width of D. The cylinder falls under the gravity field parallel to the channel walls (Figure 1). The fluid in the channel is at rest and the flow is induced by the motion of the cylinder. The fixed parameters are the ratio diameters D/d equal to 3.3 and the density ratio equal to 2.

We provide quantitatively reproducible results by specifying the relevant parameters of the problem. The simulations demonstrate the applicability of the chimera method having a strong potential for simulations of sedimenting particles.

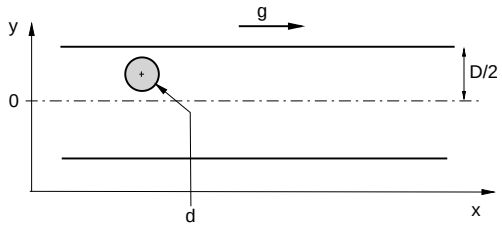

Figure 1. *Configuration of the cylinder falling in a channel*

In the first section, we provide of details the numerical method and explain the implemented fully automatic chimera method. In the second part, we discuss the validation of this numerical tool to simulate the movement of a body. In the last section, we focus on the fall of a cylinder between two walls with an interest in the influence of the number of Galileo and the initial position on trajectories.

2. Numerical method

The chimera method is used for the simulations of a moving cylinder. The chimera method is based on the very simple concept of overlapping grids (Benek *et al.*, 1983), however its implementation is quite complicated. In this study an automatic, flexible and accurate fast chimera method for moving geometries is implemented in the NSMB solver (Navier-Stocks MultiBlocks, (Vos *et al.*, 1998; Vos *et al.*, 2002)).

The first step of the chimera method is to determine the overlapped region. When dealing with huge grids or multiple overlapping grids, finding the overlapped cells is a long process. It can be done as a pre-processing step, but, when dealing with moving grids, it has to be done inside the solver. In NSMB, this operation is accelerated by using the Box algorithm of Siikonen et al. (Siikonen *et al.*, 2000). This algorithm is based on the creation of a virtual uniform cartesian grid which links mesh coordinates. Each grid point belongs to a box I,J,K of this virtual grid. Each virtual cell contains a limited number of physical grid points (overlapped or not) and the search of overlapped cells is done inside this virtual cell which is much faster than searching in the whole grid. Another issue concerns the points that are inside a solid body. In the case of a cylinder for example, the cells inside the cylinder are not overlapped but they are not fluid cells either. To remove these cells two methods are implemented : for simple cases (cylinder, sphere) we use an analytical function and for general cases, we compute the dot product of the vector from the cell center to the nearest wall cell center and of the associated wall normal vector. If the dot product is positive, the cell

is in the solid region and blanked, otherwise the cell is out of the solid region and is considered as belonging to the computational domains.

The second step of the method is to determine the nature of the overlapped regions. There are two kinds of overlapped cells : the first one is a 'donor' cell (or a 'dominant' cell) where the Navier-Stokes equation are solved, the second is the 'receptor' cell (or 'nondominant') where the state variables are obtained by interpolation from the 'donor' cells. This classification of overlapped regions has gained less attention of the researchers and in many studies, it has been simplified to the definition of an overlapped hierarchy of each block. For example, the configuration of the flow past an unconfined circular cylinder is defined by a dominant polar mesh around the cylinder over a nondominant cartesian mesh. All the cells of the polar grid are dominant over the background cartesian grid. The definition of this criterion is simple but it applies to the block as a whole and it is therefore less flexible. For a complex configuration like interactions between two walls, this criterion is unsuitable. Siikonen et al. (Siikonen *et al.*, 2000) or Liao et al. (Liao *et al.*, 2007) or (Landmann *et al.*, n.d.) proposed a criterion based on the volume of the cell. The smallest of two overlapping cells is the 'donor' and the biggest is the 'receptor'. This criterion is defined for each cell and it is more flexible than block hierarchy criterion and allows, for example, the simulation of the flow past two tandem circular cylinders in 2D. For similar overlapped meshes, this criterion works well but, for different geometries, attention must be paid to the mesh quality. For example, this criterion does not work properly in the case of the simulation of the flow past a cylinder near a plane wall. The cell aspect ratio of the near wall mesh is not the same as that of the polar wall mesh. For this reason the cell volume criterion is not sufficient.

We developed a third criterion based on the distance of a cell to the nearest local wall. The nearest local wall is the wall in the same block or the same group of blocks where the cell is defined (Figure 2). The cell which has the smallest distance to its nearest local wall is a donor cell and the other becomes a receptor. This approach guarantees the resolution of Navier-Stokes equations in the near wall region by the block to which this latter belongs and where the grid resolution is more suitable.

We use all these three criteria in our solver. The first is the hierarchy of the block. If overlapped cells have the same hierarchy, the next criterion is based on the nearest local wall distance then on the volume of the cell. The detection of donor and receptor cells is fully automatic and allows the treatment of relative moving grids.

A chimera method allows us to mesh the space with two distinct overlapped grids (Figure 3). The first one is usually a cartesian grid and spans the whole computational domain. It is refined in the proximity of walls and its defined in Cartesian coordinates. The second grid is a polar grid with a refinement close to the cylinder. The final chimera grid is a combination of both meshes. The polar mesh is defined as the dominant grid and the solution obtained on the polar grid is interpolated on the cartesian grid for the overlapped cells. The boundary conditions are classical boundary conditions for the cartesian grid with an inlet condition and outlet/wall boundary conditions. The wall boundary conditions of the polar mesh are a no-slip wall condition

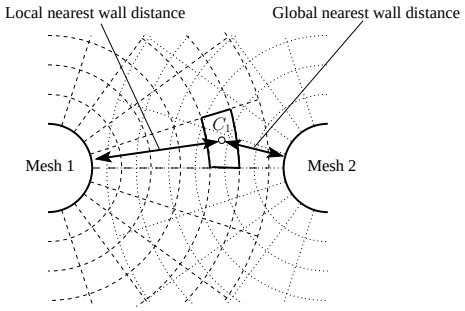

Figure 2. *Definition of local nearest wall distance and global nearest wall distance for the cell C_1 of the mesh 1 in the configuration of two overlapped polar meshes*

for the cylinder wall and a chimera boundary condition representing the link with the cartesian grid.

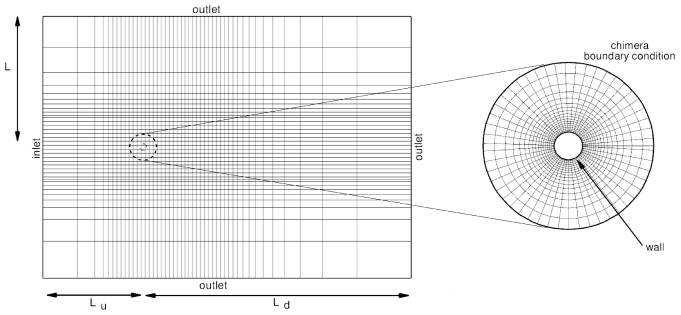

Figure 3. *Combination of a cartesian mesh and a polar mesh for a simulation of an unconfined cylinder (a 5 times coarser mesh than in the simulation is represented)*

The creation of the mesh is similar for the confined configuration. Two distinct overlapped meshes are used. The first is the polar mesh and the second is the cartesian grid with two walls. The upstream length L_u is equal to $10d$, and the downstream length L_d is equal to $25d$. The number of cells is equal to 354 964 cells. The Confined configuration does not use a basic criterion of chimera method and, in this case, the criterion of local wall distance is essential (Figure 4).

NSMB is a compressible solver with artificial preconditionner (Chorin, 1968). A second order central scheme is used for the diffusive terms and the convective terms are also discretised with a second order central scheme with artificial dissipation of Jameson (Jameson, 1995). For the time scheme, the dual time stepping scheme with backward second order interpolation is used. The system is solved with an implicit

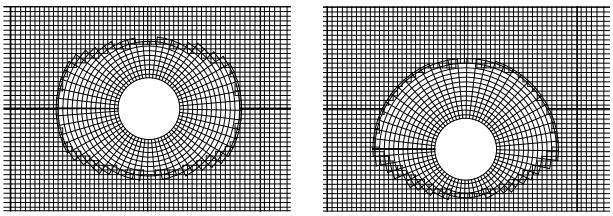

(a) (b)

Figure 4. *Automatic definition of chimera mesh for the confined configuration* $D/d = 3.3$*, and for two positions of the cylinder,* $y_0/d = 0$ *(a) and* $y_0/d = -0.65$ *(b) (a 5 times coarser mesh than in the simulation is represented)*

LU-SGS (Lower-Upper Symmetric Gauss Seidel) scheme. NSMB is fully parallelized with MPI message passing communication.

The results are decomposed into two parts. The first part concerns the validation of the moving chimera method on a moving cylinder in an infinite flow. In the second part, the flow over a moving cylinder confined by two flat walls is examined. The motion of the cylinder is compared for both the confined and unconfined configuration.

3. Validation of the chimera method for moving body

Three cases are used to validate the numerical method for moving bodies. The first case is a forced transverse oscillation of a cylinder in an infinite flow. The oscillation is defined by Equation [1] and two parameters are used for this study : A, the amplitude of the oscillations, and f/f_0, the ratio between the frequency of the imposed motion and the Von Kármán wake frequency for the fixed cylinder. Numerous publications (Koopmann, 1967; Williamson *et al.*, 1988; Anagnostopoulos, 2000; Nobari *et al.*, 2006; Placzek *et al.*, 2009) deal with this issue and the behavior of the vortex shedding is well known. Two different states are defined : the "lock-in" case where the frequency of the vortex shedding takes the frequency of the cylinder motion and the "lock-out" case where the vortex shedding has its own frequency, different from the one of the motion. In our study, only a "lock-in" simulation will be used to validate the moving chimera method.

$$y(t) = A\, sin(2\pi\ f\ t) \qquad [1]$$

The second case studied is a VIV case of a free elastic cylinder. The motion of the cylinder is modelled by a harmonic system composed of an oscillating mass (dimensionless value given by mass ratio $m = \frac{\pi\rho_b}{2\rho}$), spring (dimensionless stiffness

$k = k_{dim}/(\frac{1}{2}\rho U_\infty^2)$) and damping (nondimensionalised by $b = b_{dim}/(\frac{1}{2}\rho U_\infty^2 D)$). The system has one degree of freedom which is the translation in the vertical direction. The equation of motion of the cylinder is given by the differential equation written in dimensionless form in Equation [2]. An interaction between the fluid and the movement of the cylinder occurs. Williamson et al. (Govardhan *et al.*, 2000), Shiels et al. (Shiels *et al.*, 2001) and also recently Placzek et al. (Placzek *et al.*, 2009) have studied the different responses of the cylinder to the parameters (m, b, k). We have simulated four different cases without damping. The solution of the second order differential equation (Equation [2]) is obtained by using a Newmark algorithm with a first-order extrapolation of the lift coefficient C_y.

$$m\ddot{y} + b\dot{y} + ky = C_y(t) \qquad [2]$$

The last comparison is the free fall of a cylinder under gravity in an infinite space. The cylinder has three degrees of freedom : two translational (x and y) and one rotational (α). The movement is governed by the second law of Newton which has been nondimensionalized and written for the circular cylinder (Equation [3]). The key parameters for the falling of a body in a fluid are the density ratio (β) and the Galileo number (Ga). The coupling methodology to simulate a freely falling cylinder is a weak coupling with a first-order temporal extrapolation of the lift coefficient.

$$\ddot{x} = g\,(1-\beta) + \frac{2U_\infty^2\beta}{\pi d^2}\,C_x \;\;, \qquad \ddot{y} = \frac{2U_\infty^2\beta}{\pi d^2}\,C_y \;\;, \qquad \ddot{\alpha} = \frac{16U_\infty^2\beta}{\pi d^4}\,C_m \qquad [3]$$

The obtained results are summarized in Table 1 and they are in good agreement with the literature. For forced transverse motion of the cylinder, the vortex shedding frequency is the same as the motion frequency. The mean drag coefficient and the maximum of lift coefficient are in good agreement with Placzek et al. (Placzek *et al.*, 2009). For the freely vibrating cylinder, the amplitude and the frequency of the transverse motion characterize the motion of the cylinder. The response of the cylinder depending on the damping and mass parameters are in the good agreement with the results of Shiels et al. (Shiels *et al.*, 2001). For the last test case, the freely falling cylinder, two cases are considered. The first set of parameters $(Ga; \beta) = (12.331; 6.5)$ results in a straight fall of the cylinder and its terminal velocity is in good agreement with the value of Cruchaga et al. (Cruchaga *et al.*, 2008). When the Galileo number increases the velocity of the cylinder increases and a vortex shedding appears in the wake of the falling cylinder. The results of Namkoong et al. (Namkoong *et al.*, 2008) are available in this case for the set of parameters $(Ga; \beta) = (151; 2)$. The obtained values of the mean terminal velocity and of the Strouhal number are in agreement with the bibliographic results.

4. Free cylinder falling in a channel

In this section, the movement of a 2D cylinder falling in a channel is simulated with the chimera approach. The influence of the initial position and the Galileo number is

Table 1. *Results for the validation test cases*

		Placzek et al., 2009		Present study	
Forced motion	$(A; f/f_0)$	$\overline{C_x}$	$C_{y,max}$	$\overline{C_x}$	$C_{y,max}$
	$(0.25; 0.90)$	1.50	0.28	1.48	0.29
	$(0.25; 1.10)$	1.75	1.44	1.71	1.60
		Shiels et al., 2001		Present study	
Freely vibrating cylinder	(m, k)	A_y	f_y	A_y	f_y
	$(4; 0)$	0.05	0.16	0.05	0.166
	$(5; 4.74)$	0.46	0.16	0.454	0.153
	$(0.5; 1)$	0.56	0.19	0.554	0.188
	$(5; 9.88)$	0.57	0.2	0.565	0.197
		Cruchaga et al., 2008		Present study	
Freely falling cylinder	$(Ga; \beta)$	Re_x		Re_x	
	$(12.331; 6.5)$	7.8525		8.22	
		Namkoong et al., 2008		Present study	
	$(Ga; \beta)$	Re_x	Str	Re_x	Str
	$(151; 2)$	168.5	0.1761	167.11	0.1774

studied. The two fixed parameters are the diameter ratio (D/d) equal to 3.3 where D is the channel height and d the cylinder diameter, the density ratio ($\beta = \rho/\rho_b$) equal to 2. The varying parameters are the Galileo number Ga and the initial transverse position y_0. The range of the Galileo number studied is $151 \leq Ga \leq 300$. The results are compared to the simulation of a unconfined falling cylinder in order to determine the influence of the wall.

4.1. *Trajectories*

The trajectory for $Ga = 200$ (Figure 5) is different depending whether the cylinder is confined or not, and for the confined configuration, if the initial position is in the middle plane or not. For the unconfined falling cylinder, a deviation of the transverse position appears in the first part. In the second part of the trajectory, the transverse position oscillates around a value that is not equal to the initial transverse position. For the confined falling cylinder with $y_0 = 0$, the deviation doesn't exist and for the periodic pattern, the transverse oscillation is located around the initial value (i.e. the middle axis). For the confined falling cylinder with $y_0/d = -0.65$, the first part is different when the cylinder is placed symmetry axis. The second part of the periodic oscillation is similar to the one with $y_0 = 0$, with an oscillation around the middle axis and the same frequency and amplitude.

The temporal variation of the velocity components is represented in Figure 6. The dimensional time (t^*) is nondimensionalised with the terminal velocity U_t by the re-

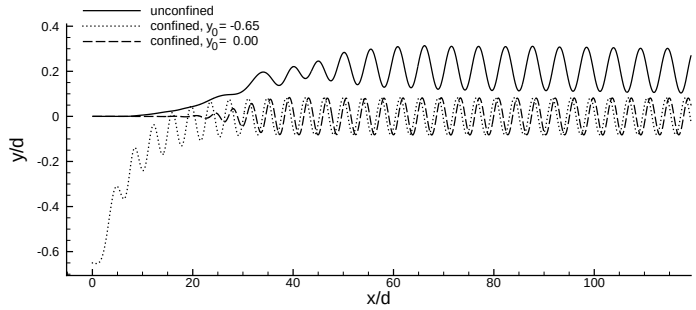

Figure 5. *Trajectories for* $Ga = 200$

lation $t = t^* d/U_t$. The behavior of the x-component is linear and dominated by the strong gravity effect. The y-component is dominated by the wake induced force. In this case, the Von Kármán vortex shedding produces a periodic oscillations. For $Ga = 200$, the amplitude of the transverse oscillation is equal to 0.09801 for unconfined configuration and 0.08155 for the both confined configurations. Those amplitudes are less than 3% of the distance between the channel walls. The confinement decreases the amplitude of the transverse oscillations but increases its frequency. We will discuss in 4.3 the correlation between the Strouhal and the Reynolds number. Moreover, the confinement fixes the axis of the oscillation to the center axis between the two walls.

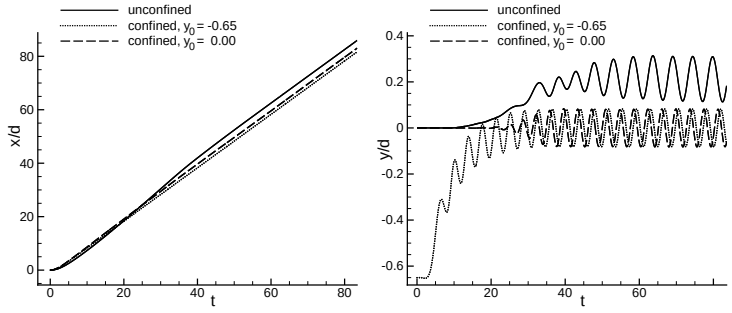

Figure 6. *Components of the position* x/d *and* y/d *versus the dimensionless time for* $Ga = 200$

4.2. *Velocities of the cylinder*

The velocity is represented by the Reynolds number $Re = U.d/\nu$, with ν the kinematic viscosity. The x-component of the velocity (gravity direction) is represented by Re_x and the y-component (transverse direction) by Re_y. The variation of Re_x is composed of three parts (Figure 7). When dropped the cylinder has no velocity and the first part is an acceleration phase with a strong increase of the falling velocity. The second step, called over-shoot, is a phase during which the increase of velocity stops and even decreases due to the the onset of the vortex shedding. This over-shoot is more visible for the unconfined falling cylinder than for the confined configuration. The last phase of the motion is a periodic oscillation of the velocity about a constant mean value ($\overline{Re_x}$).

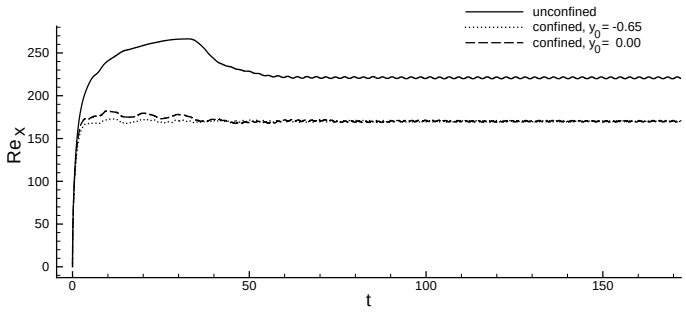

Figure 7. *X-component of the velocity defined by $Re_x = U_x d/\nu$ versus dimensionless time for $Ga = 200$*

The influence of the Galileo number on the mean terminal velocity and on its amplitude is represented in Figure 8. The amplitude of the oscillations of the velocity increases with the increase of the Galileo number in the unconfined case. To the contrary, for the confined falling cylinder, the amplitude of oscillations of the falling velocity does not increase with the increase of Galileo. The relation between the mean falling velocity and the Galileo number is practically linear. We found the relation $\overline{Re_x} = 1.092Ga + 2$ for the unconfined case and $\overline{Re_x} = 0.915Ga - 12$ for the confined cylinder. For the unconfined configuration, $Re > Ga$ and for the confined case $Re < Ga$.

The transverse velocity is represented by Re_y. The first observation is that its value is lower than 10% of the falling velocity. This velocity is just induced by the vortex shedding forces which are weaker than gravity force. The Figure 9 show the time evolution of the transverse velocity for the confined and the unconfined cylinder with $Ga = 200$. The behaviour of the transverse velocity is similar for the unconfined cylinder and for the confined configuration with an initial position at tha middle axis. Oscillations increase progressively and these oscillations appear faster in the confined case. For the confined configuration with an initial position out the middle

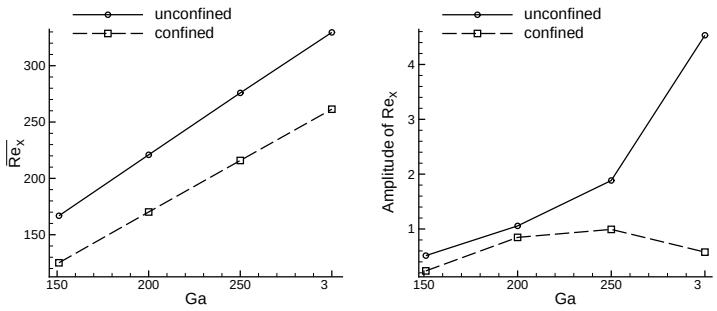

Figure 8. *$\overline{Re_x}$ and amplitude of Re_x versus Galileo number for a confined and an unconfined falling cylinder and for $Ga = 200$*

axis ($y_0/d = -0.65$), the oscillations appear immediately with an amplitude close to the final amplitude. The wall effect creates an asymmetric geometry, a powerful force appears, and the asymmetric geometry facilitates the onset of the vortex shedding.

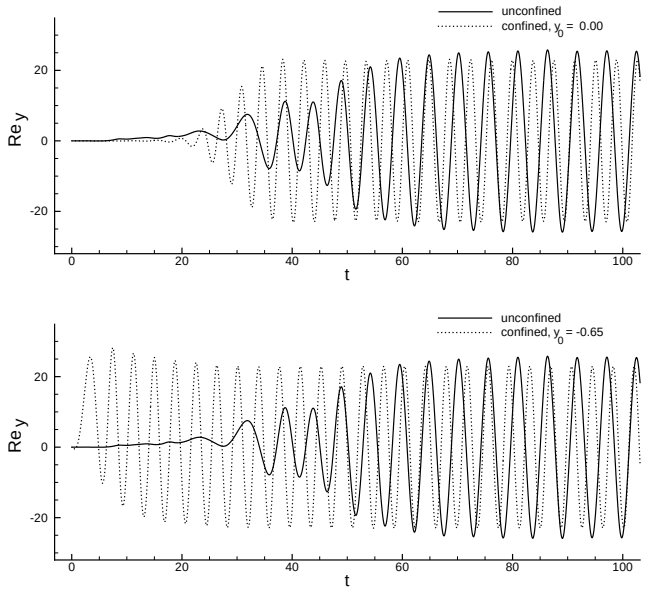

Figure 9. *Y-component of the velocity defined by $Re_y = U_y d/\nu$ versus dimensionless time for $Ga = 200$*

The evolution of Re_x and Re_y versus the transverse position y/d for the falling cylinder in the unconfined and confined cases for $Ga = 200$ during the periodic state is presented in (Figure 10). The maximum of the transverse velocity appears when the cylinder is on the mean transverse position and the transverse velocity is equal to zero when the cylinder is at the extreme position of the motion. The behaviour of the falling velocity is opposite with a maximum velocity for the extreme position, and minimum velocity when the cylinder is at the mean position. The variation of the angular velocity is different and the maximum appears for $1/4$ of the maximum displacement.

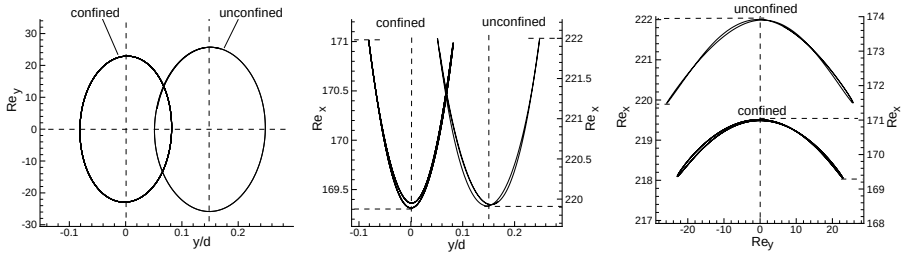

Figure 10. *Relation between velocity (Re) and position (y/d) and between the translation velocities for $Ga = 200$*

4.3. *Frequencies of the falling cylinder*

The frequency defined by the Strouhal number ($St = fd/U_x$) was first linked to the Reynolds number by Williamson et al. (Williamson *et al.*, 1998) for the fixed cylinder by the following function :

$$St = A + \frac{B}{\sqrt{Re}} + \frac{C}{Re} \qquad [4]$$

This function can be simplified with $C = 0$ for the range of Reynolds number $Re < 188$. With the present results, the coefficients are determined and we have obtained the following coefficients :

$$\text{unconfined :} \quad St = 0.2086 + \frac{0.0548}{\sqrt{Re}} - \frac{5.9004}{Re} \qquad [5]$$

$$\text{confined :} \quad St = 0.2527 + \frac{0.8581}{\sqrt{Re}} - \frac{9.3165}{Re} \qquad [6]$$

$$\text{fixed cylinder :} \quad St = 0.27661 - \frac{1.1129}{\sqrt{Re}} - \frac{0.4821}{Re} \qquad [7]$$

The fitted functions and the data are plotted in Figure 11. The behavior of the the Strouhal number is well represented by the function [4]. The confinement accelerates the oscillation and the frequency is higher. The difference with the unconfined case is significant. The flow in the gap between the wall and the cylinder is more accelerated and drives the vortex out more rapidly.

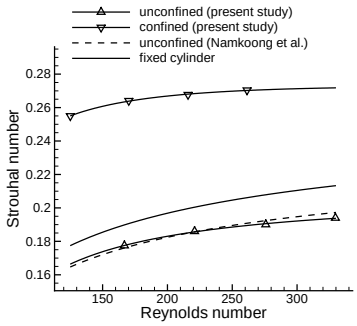

Figure 11. *Data and fitted functions of the Strouhal number versus Galileo number*

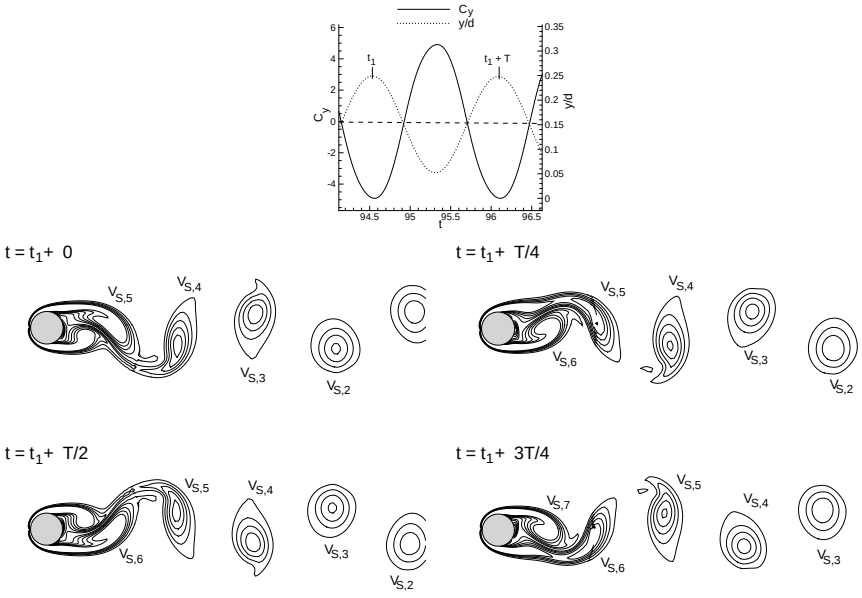

Figure 12. *Isovorticities for unconfined falling cylinder and for* $Ga = 200$

4.4. *Structure of the flow*

The wake of the cylinder is due to the motion of the cylinder. The speed of the cylinder is such that the vortices at the rear of the cylinder are not steady but they are detached periodically resulting in the Von Kármán vortex shedding. This vortex shedding induces the oscillation of the position. In the unconfined case for $Ga = 200$, we choose the starting time t_1 when the cylinder is at the maximum transverse position and we examine the vortex structures over one period of oscillation (Figure 12). The transverse position is directly linked to the vortex shedding. At the time $t = t_1$, the vortex $V_{S,5}$ is ejected from the cylinder. This vortex is a clock-wise vortex with negative vorticity. At this time the lift is minimum. Then the vortex $V_{S,6}$ grows. It's a counter clock-wise vortex associated to positive vorticity and due to viscous effects it will attract the cylinder to it so that the cylinder will move to a negative y position. As a result of this positive vorticity the lift increases. At the time $t = t_1 + T/4$, the cylinder is at the axis. At the time $t = t_1 + T/2$ the vortex $V_{S,6}$ is ejected, the lift is maximum and the cylinder has reached its minimum position. The vortex $V_{S,7}$ grows. The negative associated vorticity will attract the cylinder to positive y positions. Again at $t = t_1 + 3T/4$ the cylinder crosses the y axis, the lift is zero.

5. Conclusion

We have implement a fast and efficient automatic chimera method for the simulation of flow around moving bodies. This method allows for a relative motion of a mesh over a second one thanks to data interpolation at the overlapped boundaries. This method was validated on three different body motions (forced motion, elastic motion and free motion), and the results are in good agreement with the literature. This method was then used to simulate the fall of a circular cylinder in a channel under the action of a gravity field parallel to the wall plates. The parameters characterising the problem, (Ga, β), are chosen in order to obtain vortex shedding in the wake of the falling cylinder. The range of the studied Galileo numbers is $151 \leq Ga \leq 300$ and the density ratio is fixed to 2. The effects of the presence of walls are : a decrease of mean terminal vertical velocity, a light decrease of the transverse motion amplitude, a decrease of the over-shoot and a radical increase of the frequency of the motion. The initial position determines the transients but not the periodic terminal motion. In the case of the cylinder dropped out the middle axis, the transverse oscillation appears almost immediately with the amplitude close to the terminal amplitude. For all periodic motions, the transverse motions are in opposite phase to the vortex shedding.

6. References

Anagnostopoulos P., " Numerical study of the flow past a cylinder excited transversely to the incident stream. Part 1: Lock-in zone, hydrodynamic forces and wake geometry", *Journal of Fluids and Structures*, vol. 14, p. 819-851, 2000.

Benek J. A., Steger J. L., Dougherty F., " A flexible grid embedding technique with application to the Euler equations", *AIAA Paper*, 1983.

Braza M., Chasaing P., Ha Minh H., " Numerical study and physical analysis of the pressure and velocity fields in the near wake of a circular cylinder", *Journal of Fluid Mechanics*, vol. 165, p. 79-130, 1986.

Chorin A., " Numerical solution of the Navier-Stokes equations.", *J. Math. Computation*, vol. 22, p. 745, 1968.

Cruchaga M., Muñoz C., Celentano D., " Simulation and experimental validation of the motion of immersed rigid bodies in viscous flows", *Computer Methods in Applied Mechanics and Engineering*, vol. 197, p. 2823-2835, 2008.

Dušek J., Le Gal P., Fraunié; P., " A numerical and theoretical study of the first Hopf bifurcation in a cylinder wake", *Journal of Fluid Mechanics*, vol. 264, p. 59-80, 1994.

Feng J., Hu H., Joseph D., " Direct simulation of initial value problems for the motion of solid bodies in a Newtonian fluid Part 1. Sedimentation", *Journal of Fluid Mechanics*, vol. 261, p. 95-134, 1994.

Govardhan R., Williamson C., " Modes of vortex formation and frequency response of a freely vibrating cylinder", *Journal of Fluid Mechanics*, vol. 420, p. 85-130, 2000.

Horowitz M., Williamson C., " Dynamics of a rising and falling cylinder", *Journal of Fluids and Structures*, vol. 22, p. 837-843, 2006.

Jameson A., " Analysis and design of numerical scheme for gas dynamics, 1 : artificial diffusion, upwind biased, limiters and their effect on accuracy and multigrid convergence", *Computational Fluid Dynamics*, 1995.

Jenny M., Dušek J., " Efficient numerical method for the direct numerical simulation of the flow past a single light moving spherical body in transitional regimes", *Journal of Computational Physics*, vol. 194, p. 215-232, 2004.

Koopmann G. H., " The vortex wakes of vibrating cylinders at low Reynolds numbers", *Journal of Fluid Mechanics*, vol. 28, p. 501-512, 1967.

Landmann B., Montagnac M., " A highly automated parallel Chimera method for overset grids based on the implicit hole cutting technique", *International Journal for Numerical Methods in Fluids*, n.d.

Liao W., Cai J., Tsai H. M., " A multigrid overset grid flow solver with implicit hole cutting method", *Computer Methods in Applied Mechanics and Engineering*, vol. 196, p. 1701 - 1715, 2007.

Namkoong K., Yoo J., Choi H., " Numerical analysis of two-dimensional motion of a freely falling circular cylinder in an infinite fluid", *Journal of Fluid Mechanics*, vol. 604, p. 33-53, 2008.

Nobari M., Naderan H., " A numerical study of flow past a cylinder with cross flow and inline oscillation", *Computers & Fluids*, vol. 35, p. 393-415, 2006.

Persillon H., Braza M., " Physical analysis of the transition to turbulence in the wake of a circular cylinder by three-dimensional Navier-Stokes simulation", *J. Fluid Mech.*, vol. 365, p. 23-88, 1998.

Placzek A., Sigrist J., Hamdouni A., " Numerical simulation of an oscillating cylinder in a cross-flow at low Reynolds number: Forced and free oscillations", *Computers & Fluids*, vol. 38, p. 80-100, 2009.

Shiels D., Leonard A., Roshko A., " Flow-induced vibration of a circular cylinder at limiting structural parameters", *Journal of Fluids and Structures*, vol. 15, p. 3-21, 2001.

Siikonen T. L., Rautaheimo P. P., Salminen E. J., " Numerical techniques for complex aeronautical flows", *European Congress on Computational Methods in Applied Sciences and Engineering ECCOMAS 2000*, 2000.

Tritton D., " Experiments on the flow past a circular cylinder at low Reynolds numbers", *Journal of Fluid Mechanics*, vol. 6, p. 547-567, 1959.

Vos J., Rizzi A., Darracq D., Hirschel E., " Naviers-Stokes solvers in European aircraft design", *Progress in Aerospace Sciences*, vol. 38, p. 601-697, 2002.

Vos J., Rizzi A., orjon A., Chaput E., Soinne E., " Recent Advances in aerodynamics inside the NSMB (Navier-Stokes Multiblock) Consortium", *AIAA paper*, 1998.

Williamson C., Brown G., " A series in $1/\sqrt{}$ Re to represent the Strouhal–Reynolds number relationship of the cylinder wake", *Journal of Fluids and Structures*, vol. 12, p. 1073-1085, 1998.

Williamson C., Roshko A., " Vortex formation in the wake of an oscillating cylinder", *Journal of Fluids and Structures*, vol. 2, p. 355-381, 1988.